Increased photo-stability of quantum dots in segregated bilayer films

G. V. Shcherbatyuk, P. Talbot, J. Mandal, A. J. Krejci, J. H. Dickerson' , and S. Ghosh'

Citation: Journal of Applied Physics **114**, 084305 (2013); doi: 10.1063/1.4819090
View online: http://dx.doi.org/10.1063/1.4819090
View Table of Contents: http://aip.scitation.org/toc/jap/114/8
Published by the American Institute of Physics

Increased photo-stability of quantum dots in segregated bilayer films

G. V. Shcherbatyuk,[1] P. Talbot,[1] J. Mandal,[2,3] A. J. Krejci,[2,3] J. H. Dickerson,[2,3,4,a)] and S. Ghosh[1,a)]

[1]*Department of Physics, University of California, Merced, California 95343, USA*
[2]*Department of Physics and Astronomy, Vanderbilt University, Nashville, Tennessee 37235, USA*
[3]*Vanderbilt Institute for Nanoscale Science and Engineering, Vanderbilt University, Nashville, Tennessee 37235, USA*
[4]*Department of Chemistry, Vanderbilt University, Nashville, Tennessee 37235, USA*

(Received 15 May 2013; accepted 6 August 2013; published online 26 August 2013)

We report a comparative study of photo-stability of CdSe/ZnS quantum dots (QDs) in a variety of thin film samples. These include electrophoretically deposited single and differently sized segregated bilayer films and self-assembled mixed-sized films. Our studies follow static and dynamic QD photoluminescence over prolonged periods of photo-excitation and find that compared to both single-sized and mixed-sized films, the segregated bilayer samples exhibit highest photo-stability. These films show a QD emission quench rate of ~2.5 times slower than the others and have almost negligible spectral shifts (<2 nm). Time-resolved measurements indicate very short inter-layer energy transfer (ET) time for the acceptor QDs in the bilayer, coupled with low ET efficiency for the donor dots. Further analysis reveals a complex interplay of intra- and inter-ensemble ET, with ET rates that have disparate spectral dependence between the mixed and bilayer films, and we conclude that this leads to the enhanced photo stability in the latter. Our findings provide a vital clue to the optimal design of QD based energy-harvesting structures.
 [http://dx.doi.org/10.1063/1.4819090]

I. INTRODUCTION

The many advantages of chemically synthesized semiconducting quantum dots (QDs) are well-documented,[1–6] primary among which are the size-tunability of the energy band-gap arising from quantum confinement and the broad absorption spectrum. The latter characteristic is particularly advantageous for application in solar energy harvesting devices. Considerable research has also explored the deterioration of QDs[7–9] with time, which severely limit the shelf-life such devices might have. Typically, an ensemble of QDs exhibit emission quenching under prolonged photo-excitation, often accompanied by the emission shifting to shorter wavelengths (blue-shift) as a result of oxidation of the QD core. These changes are additionally reflected in increased recombination rates as the defect states that cause emission quenching act as non-radiative recombination traps. Efforts to increase QD resistance to photo-oxidation and to stabilize the emission by tuning intrinsic structural properties have also been reported.[10–12]

We are investigating the role that inter-QD energy transfer (ET) plays in photo-induced effects. The mechanism by which smaller QDs transfer energy to larger ones has been established as the familiar Förster resonant energy transfer (FRET) method,[13] strongly dependent on the spectral overlap of the involved entities and their inter-particle separation. Our prior studies indicated that while the intra-ensemble FRET among mono-dispersed QDs[14] leads to faster emission quenching on photo-exposure (also referred to as photo-darkening), a mixture of two differently sized QDs in an almost equal ratio reduce both darkening and oxidation in the smaller QDs, which act as the donors for FRET.[15] Here, we present results obtained on electrophoretically deposited monolayer (ML) and bilayer (BL) structures. The BL films are segregated, where each layer consists of QDs of one size. We compare the results to those obtained in mixed film (MF) samples. A MF sample is created by first mixing two differently sized QDs (donors and acceptors) in solution, and then allowing a self-assembled film to form by drop casting method. In such a sample, the energy transfer between QDs has no directionality and is confined in the plane of the film, while in a BL sample, energy transfer occurs in a specific direction, from the donor layer to the acceptor. We observe greatly reduced emission quenching and oxidation rates in both donor and acceptor QDs in the BL samples, compared to both the MF samples and the monolayer control samples.

II. EXPERIMENTAL DETAILS

We use CdSe/ZnS core-shell QDs suspended in hexane (Ocean Nanotech, Inc.) to fabricate our samples by electrophoretic deposition.[16,17] Colloidal suspensions of the QDs are prepared by diluting the as received material in 10 ml of hexane. The QDs deposit onto indium tin oxide substrates ($R_s = 15–25\ \Omega$; Delta Technologies), separated by a 5 mm gap in a parallel-plate capacitor configuration. An applied voltage of 1000 V across the electrodes, employed for approximately 10 min, yields the monolayer of QDs. Subsequent insertion of the electrodes into a different suspension of QDs allows for the fabrication of bilayers.[18,19] The donor (larger band gap) dots have their emission centered on 584 nm and a core diameter of 3.2 nm, while the acceptor (smaller band gap) QDs are 5.6 nm in diameter and

a)Authors to whom correspondence should be addressed. Electronic addresses: sghosh@ucmerced.edu and james.dickerson@vanderbilt.edu

emit at 620 nm. Our photo-excitation sources include a continuous wave diode laser emitting at 405 nm for static spectroscopy, and a pulsed and frequency-doubled Ti:sapphire laser tuned to 405 nm for time-resolved photoluminescence (PL) measurements. For both measurements, the average incident laser power used is $<150\ \mu$W, where the QD emission properties are independent of excitation power. The samples are mounted on our custom-built scanning confocal microscope with a 500 nm spatial resolution. The PL is dispersed by a spectrometer onto a thermo-electrically cooled CCD, a system that has a spectral resolution of 0.18 nm in the wavelength range of our samples. For absorption spectroscopy, we use a UV-VIS spectrophotometer. All measurements are performed at room temperature under ambient conditions.

III. RESULTS AND DISCUSSION

Figure 1 summarizes the photo-excitation studies on a monolayer sample with just the acceptor QDs (A-ML). After a rapid brightening in the initial few minutes, this sample exhibits considerable PL quenching in the given 120 min period, as seen in Fig. 1(a). Using an exponential decay to model a numerical quench rate, we find that A-ML has a 1/eth decay time of 20 min and loses approximately 70% of its initial intensity by the end. Fig. 1(a) also shows the corresponding emission peak wavelengths (λ_{PEAK}) evolving with time. The sample exhibits a large red-shift of 7 nm from its emission in solution at the start, which decreases slowly over the same

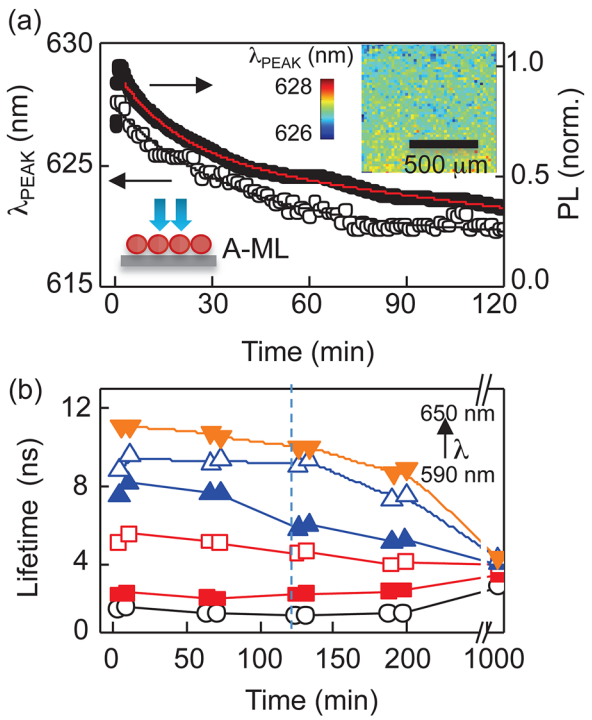

FIG. 1. Static and dynamic spectral evolution of acceptor QDs with photo-excitation. (a) Emission intensity (solid circles) and emission wavelength (open circles) varying with excitation time for acceptor monolayer shown in the schematic. Lines are exponential fits. (Inset) Spatially resolved scan of peak emission wavelength. (b) Spectrally resolved recombination lifetimes as functions of excitation time, taken from 590 nm (open circles) to 650 nm (open triangles) at 10 nm intervals. Dashed line indicates 120 min mark.

time scale as the intensity quench. Transmission electron microscopy (TEM), acquired with a Philips CM 20 transmission electron microscope operating at 200 kV, allows us to verify that the QDs are close-packed in our samples. This usually leads to intra-ensemble FRET causing red-shifted emission. A spatially resolved PL scan of λ_{PEAK} in Fig. 1(a) (inset) verifies that prior to exposure to continuous excitation the sample emission is very uniform and limited to the range of 626–628 nm. The photo-brightening observed at the start routinely occurs in QD ensembles.[20–24] PL quenching over time is also typical in QD ensembles, which has been attributed to a reversible photo-darkening analogous to collective "blinking," and an irreversible photo-oxidation, which causes a structural change by reducing the QD core size.[20–24] These effects are dependent on QD concentration, and further complicated by the presence of inter-QD energy transfer[15] in close-packed films, such as these. As in the given time the A-ML sample does not exhibit a λ_{PEAK} less than in solution, we conclude that the QDs do not oxidize rapidly. For FRET efficiency and further insight into its evolution and its role in the PL quench, we plot the recombination times of the samples in Fig. 1(b).

The lifetimes are extracted from spectrally resolved, time-resolved PL curves between 590 nm and 650 nm, at 10 nm intervals. In solution, the QD PL decays exponentially with a wavelength-independent decay time of 11 ns. In the films, inter-dot interactions result in a distribution as seen in Fig. 1(b), with the recombination times increasing with wavelength, another consequence of FRET in conjunction with λ_{PEAK} red-shift. This effect is quantified as FRET efficiency $\varepsilon = 1 - \tau_{FA}/\tau_{SA}$ (Ref. 25), where τ_{FA} and τ_{SA} are the acceptor dot recombination times in the film and in solution, respectively. In A-ML, the maximum ε calculated for the shortest wavelength is 84.5%, which remains almost unchanged in the 120 min photo-excitation period. This consistently high rate of energy transfer from the small to the large dots results in preferential darkening of the latter, which corresponds to the emission shifting to shorter wavelengths concurrently [Fig. 1(a)]. The recombination rates in Fig. 1(b) for the same period remain nominally unchanged. Prolonging the photo-excitation beyond 120 min shows a trend where the wavelength dependent distribution appears to be slowly collapsing, a result of photo-oxidation, which become considerable by 16 h and causes the entire ensemble to have PL lifetimes within a narrow range centered on 4 ns. Oxidation of the QD not only results in the core diameter decreasing but also causes surface defects that introduce energy traps within the band-gap that act as non-radiative recombination centers, explaining the faster rates of most of the dots. The smallest QDs show a slightly decreased rate due to ceasing of FRET.

Figure 2 summarizes the photo-excitation studies on donor only monolayer (D-ML) and bilayer (D-BL) samples. Both exhibit PL quenching [Fig. 2(a)] without any initial brightening. D-ML has a 1/eth decay time of 23 min, and loses approximately 80% of its initial intensity by the end. D-BL PL quenches almost entirely, with a very rapid decay within the first 1.3 min when 66% of its initial intensity is lost, while the remaining signal decays over the next 20 min.

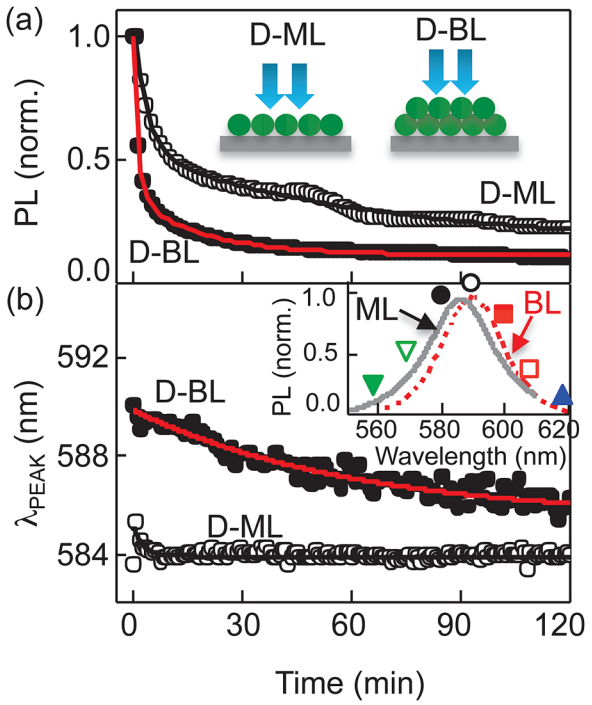

FIG. 2. (a) Emission intensity as a function of time for donor monolayer (D-ML, open circles) and bilayer (D-BL, solid circles), described by the inset schematics. (b) Emission peak wavelength varying with excitation time. Lines are exponential fits; (inset) typical emission spectra for the samples. The symbols designate the corresponding wavelengths for the time-resolved data in Fig. 3.

Fig. 2(b) (inset) confirms intra-ensemble FRET, with λ_{PEAK} red-shifted from the solution emission of 584 nm for both samples. λ_{PEAK} in D-ML [Fig. 2(b)], which shows a very small red-shift, quickly settles to the solution emission wavelength within the first few minutes. D-BL exhibits a larger initial red-shift, followed by a slow decrease. As in the case of the A-ML sample, neither donor films exhibits signs of severe photo-oxidation. The recombination lifetimes extracted from spectrally resolved, time-resolved PL curves for D-ML at wavelengths indicated by the symbols in Fig. 2(b) (inset) are plotted in Fig. 3(a), as a function of excitation time. The maximum ε is 80%, which subsequently drops to 73% by the end of the 120 min photo-excitation period. In comparison, D-BL (data not shown) has a higher initial ε of 84% that falls slightly to 80%. The consistently higher ε originates in the bilayer arrangement, because instead of the typical d^{-6} scaling with inter-particle separation d, FRET falls off slower as d^{-4} in the case of an emitter coupling to others in another plane (as in a layered structure). Higher FRET in D-BL, which accounts for the higher $\lambda_{PEAK} = 589$ nm at the start of photo-excitation, also drives the faster PL quench,[15] where the larger QDs undergo rapid darkening, showing up as an overall drop in intensity [Fig. 2(a)] and a continuous shift to lower wavelengths [Fig. 2(b)]. Fig. 3(b) follows the intra-ensemble donor-to-donor FRET rate, defined as $\kappa_F^{D-D} = 1/\tau_{FD} - 1/\tau_{SD}$, where τ_{FD} and τ_{SD} are the donor recombination times in film and in solution. Plotted with varying emission wavelength at different excitation times, κ_F^{D-D} is expectedly higher on the short wavelength side that represents the larger dots in the ensemble, and decreases with time as the larger dots darken.

Both acceptor and donor monolayer samples show similar time evolution of PL quench, while the donor bilayer quenches much more rapidly. These results suggest that intra-ensemble FRET is a deterrent to QD longevity, confirming prior similar observations in self-assembled QD samples.[15] The scanning electron microscope (SEM) image of D-A BL in Fig. 4(a) shows good coverage. To assess the inter-dot spacing within our monolayers and bilayers, we analyzed the analogous spacing within sub-monolayer films fabricated from nanoparticles that were deposited directly onto TEM grids. These TEM grid-deposited films allowed us to acquire higher resolution electron images of the films, as seen in Fig. 4(b), inset, than we acquired for our monolayer and multilayer films on ITO, analyzed through SEM [Fig. 4(a)]. The specific image analysis of the films was performed by measuring the statistical average of the radial distribution function (RDF) from the centers of all of the nanoparticles existing within the film.[25] The RDF describes how the density of particles varies as a function of distance from a particular reference nanoparticle.[26–30] The details of how we calculated the primary peak values of the radial distribution function are described elsewhere.[31] The first peak in the RDF was fit to a Gaussian distribution in Fig. 4(b); the mean value of this peak corresponded to an inter-nanoparticle spacing of 9.1 ± 0.6 nm. Given the notable spacing between the QDs, quantum effects are not likely to be observed.[32] Spatially resolved PL maps of the same area of the D-A BL sample in Fig. 4(c) show uniform emission from both types of QDs over the entire scanned region of $250 \times 250\ \mu m^2$. A representative spectrum, shown in Fig. 4(d), is overlaid with the absorption of the D-A BL, and compared to emission spectra from all the prior samples. The donor emission of D-

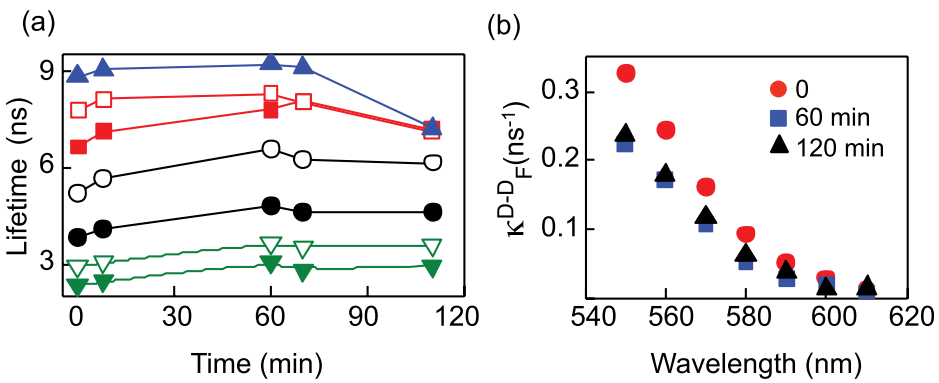

FIG. 3. (a) Spectrally resolved recombination lifetimes as functions of excitation time for D-ML. The symbols corresponding to wavelengths, as shown in Fig. 2(b) (inset); (b) FRET rate κ_F^{D-D} for the same sample, plotted as a function of emission wavelength at different times.

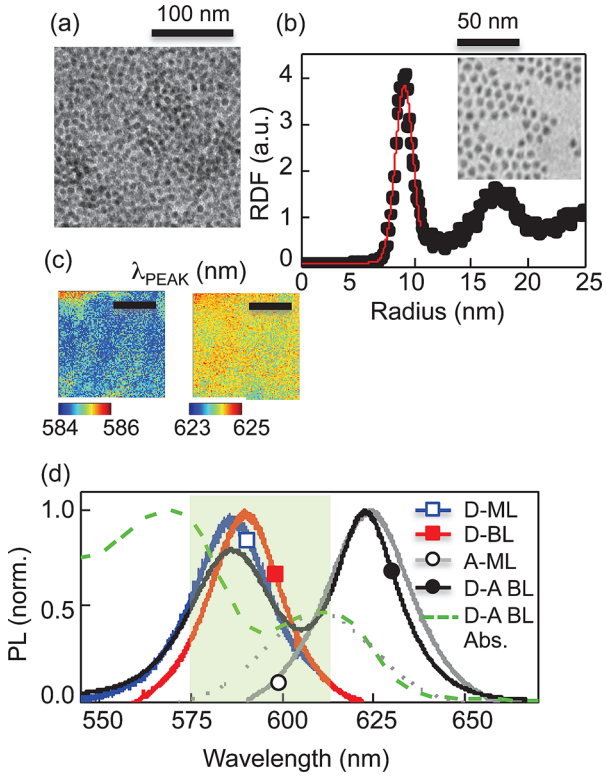

FIG. 4. (a) SEM image of bilayer sample (D-A BL). (b) (Main) RDF of the inter-dot separation; (inset) TEM image of QD layer. (c) Peak emission wavelength plotted over a 250 × 250 μm^2 area showing uniform coverage of (left) donor and (right) acceptor QDs. Scale bars represent 100 μm. (d) Emission spectra of D-A BL compared to others and to the D-A BL absorption (green dashed curve). The dotted gray curve is a fit to acceptor absorption in D-A bilayer. Shaded region highlights spectral range over which donor emission and acceptor absorption has substantial overlap.

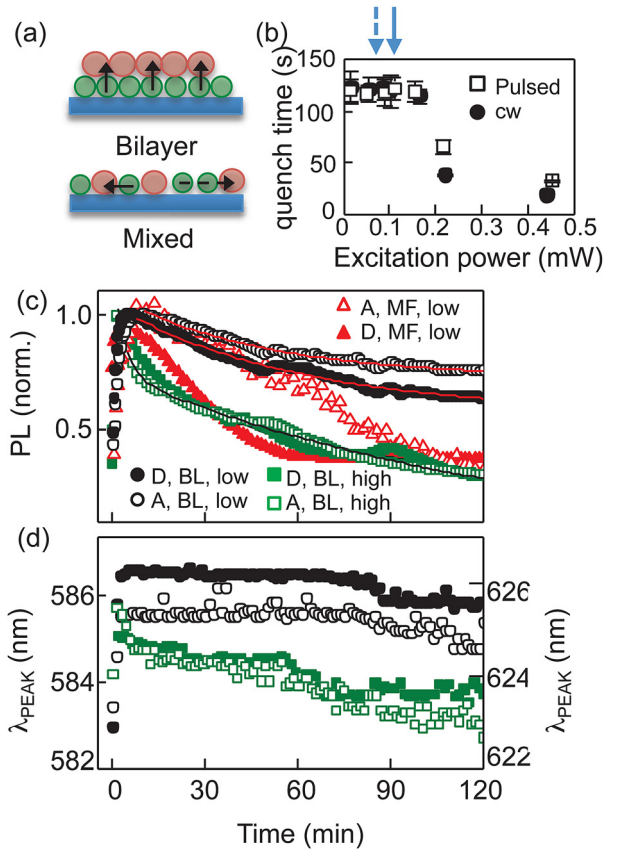

FIG. 5. (a) Schematics of bilayer and mixed film samples with donors and acceptors; the arrows show direction of FRET to acceptor QDs: direct (solid) and multistep (dashed). (b) Donor QD PL quench as a function of excitation power. (c) Emission intensity as a function of time at low and high excitation powers, superimposed on data from a D-A mixed film (MF) sample. Lines are exponential fits. (d) Emission peak wavelength varying with time for the bilayer (D-A BL) sample.

A BL is not red-shifted by much compared to the D-ML film, implying there is less intra-ensemble FRET among the donors, than observed in the D-BL sample. The acceptor emission is strongly red-shifted and equivalent to the A-ML sample; however, this phenomenon is likely due to inter-ensemble FRET in addition to some within the acceptor subset.

Fig. 5(a) shows comparative schematics of the bilayer sample (D-A BL) and a MF sample, both with donors and acceptors. Fig. 5(b) plots the PL quench rate of donor QDs, obtained from fits similar to those in Figs. 1(a) and 2(a), as a function of average excitation power for both the cw and pulsed lasers. The arrows at 110 μW (solid) and 85 μW (dashed) represent the powers used for typical static and dynamic PL measurements for our samples, respectively. We subject this sample to the same photo-excitation protocol as the others and plot the PL intensity and wavelengths in Figs. 5(c) and 5(d), respectively. At the typical low power used for all measurements so far (110 μW), donor and acceptor dots show PL quench rates [Fig. 5(c)] that are slower by factor of ~2.5 than those observed in donor and acceptor only samples. Additionally, these quench rates are slower than what is observed in MF samples, using the same excitation power, although both samples show equivalent brightening at the very beginning. The donor quench rate difference is particularly noticeable between the mixed and bilayer films. For D-A BL, increasing the excitation power to 200 μW yields a quench rate as fast as that observed for donors in the MF sample. The acceptors quench slower in the MF sample at first, but then speed up and the total emission intensity drops by more than 50% by the end, similar to the donor intensity change. In D-A BL, their quench rate, though faster than the donors, is still an improvement on the MF sample. Fig. 5(d) shows the variation of λ_{PEAK} for donors and acceptors at high and low power for D-A BL. At low excitation intensity, the emission for both appears almost constant, shifting to the blue by less than 2 nm; the emission is far more stable than what is observed in the films consisting only of one type of QD. At high power, both dots show a steady blue-shift, but for the donors the spectral peak shifts to below the solution wavelength, implying a strong influence of photo-oxidation causing increased quantum confinement. This is typical at higher excitation powers when all photo-induced effects progress faster,[15] also shown in Fig. 5(b).

In MF samples, the donor stability is enhanced when donors and acceptors are present in almost equal numbers, but acceptor performance is worse than in single-sized acceptor samples.[16] However, in the D-A BL film, emission intensity and peak wavelengths are steadily unvarying for both donors and acceptors over the measurement time-scale. To understand the cause behind the improved performance,

we look at the recombination dynamics. Figs. 6(a) and 6(b) show the decay lifetimes for the MF and BL samples, respectively, as they evolve with time for the duration of the excitation. We use multi-exponential fits to time-resolved PL data $A(t) = \sum_i A_i e^{-t/\tau_i}$, where A_i and τ_i are the intensity and characteristic time-scales representing different recombination channels. The plotted lifetimes are intensity-averaged values,[14,15,33] calculated as $\sum_i A_i \tau_i^2 / \sum_i A_i \tau_i$. In the acceptor emission range (>600 nm, unshaded region), the recombination times show similar trends in both as in the single sized QD film, with decay rates increasing steadily with time as FRET and oxidation introduces additional channels of non-radiative recombination. For the donors (<600 nm, shaded region), the PL lifetimes appear almost unchanged in the MF sample, whereas an apparent increase exists in the BL film. An additional difference between the dynamic processes in the two types of QD films is seen in Fig. 6(c), which shows representative recombination decay curves at 640 nm for both. We observe that the shapes are very different at the start of photo-excitation. The MF sample exhibits an initial increase for ~2 ns, which is not observed in the D-A BL film. This short duration rise is often referred to as a "charging" time as it provides an indication of the time over which donors keep pumping energy/carriers into the acceptors. The absence of a noticeable charging time for D-A BL implies that said charging time is much faster than in the MF sample, possibly on the scale of tens of picoseconds. The reason is outlined in Fig. 4(a), which shows that energy transfer to acceptors is occasionally a multi-step process in the MF samples when a smaller donor first transfers energy to a larger donor, which in turn transfers to an acceptor. In the BL film, the close proximity of acceptors to every donor bypasses this problem, making the process faster, although not necessarily more efficient. Fig. 6(b) (inset) shows the FRET efficiency for both samples in the entire donor emission spectral range. For the region corresponding to the most relevant spectral range for donor-to-acceptor FRET commensurate with Fig. 4(d), efficiency is lower for the BL sample, except in the very long wavelength edge (>600 nm).

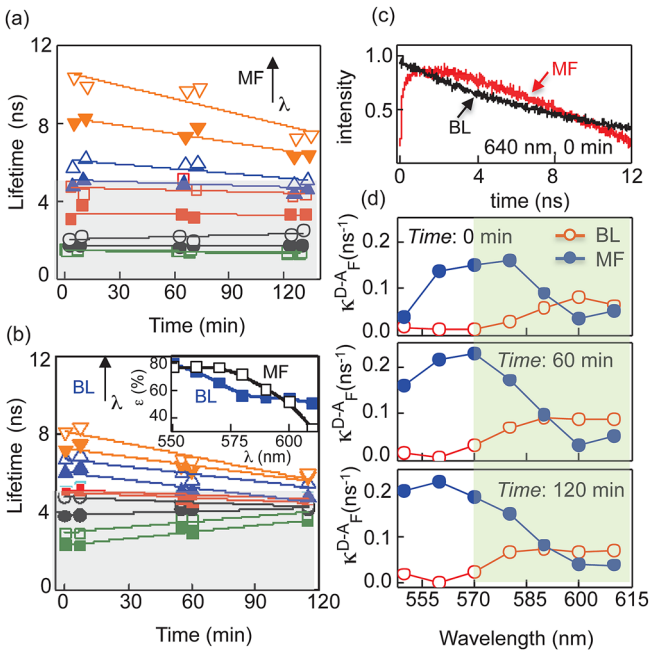

FIG. 6. Spectrally resolved recombination lifetimes as functions of excitation time for (a) D-A mixed film sample and (b) D-A bilayer sample. Data shown from 550 nm to 640 nm at 10 nm intervals, with shaded region representing donor data. (Inset) FRET efficiency ε for bilayer (BL, solid squares) and mixed film (MF, open squares) samples. (c) Representative time-resolved PL curves at 640 nm for each sample. FRET rate κ_F^{D-A} for bilayer (BL, open circles) and mixed film (MF, filled circles) samples at (top) 0 min, (middle) 60 min, and (bottom) 120 min, after excitation commences. Shaded regions in all three correspond to shaded spectral region in Fig. 4(d).

The faster energy transfer in the BL films to the acceptors appears contradictory with the lower efficiency values for the donors. The problematic issue is in the fundamental definition of FRET efficiency, which was developed in the context of isolated donor-acceptor pairs in mind. In reality, the measured donor lifetimes used to calculate the efficiencies are a reflection of recombination due to both intra- and inter-ensemble energy transfers. A better interpretation[33] that allows us to separate these two effects is calculation of FRET rate, but with a modification. The donor-to-acceptor FRET rate is defined as: $\kappa_F^{D-A} = 1/\tau_{FDA} - 1/\tau_{SD}$, where τ_{FDA} is the donor lifetime in the bilayer film τ_{FDA} and τ_{SD} is the intrinsic donor lifetime as described before. In place of τ_{SD} as measured in solution that corresponds to isolated donors that only take into account the radiative and non-radiative recombination rates, we modify κ_F^{D-A} to include the donor-to-donor FRET rate κ_F^{D-D} in addition to τ_{SD}. This rate, calculated for both BL and MF samples, is shown in Fig. 6(d) for three different times during photo-excitation. At 0 min, the MF sample has high κ_F^{D-A} in the lower side of the donor emission, which means the intra-ensemble ET rate is larger than the control donor-only sample. Conversely, κ_F^{D-A} is low for wavelengths >585 nm, implying low inter-ensemble FRET. With time, κ_F^{D-A} shifts to lower wavelengths in the MF sample. By contrast, the BL film has almost zero κ_F^{D-A} in the wavelength range where intra-ensemble FRET is dominant, but shows a stronger signature of donor-acceptor FRET. Additionally, this wavelength dependence remains unchanged over time. Donor emission is stabilized in both MF and BL samples compared to donor-only films, because they can pump carriers into acceptor dots, which allows the donors to stay dark between excitation pulses for longer. Further, lower intra-ensemble FRET in BL film enhances the donor stability more than in the MF sample, where the donor quenching is reflected in the shift of κ_F^{D-A} to lower wavelengths. The additional difference between the two samples is in the acceptor behavior since unlike in the MF sample, in the BL film they stabilize just as well as the donors. This is attributable to the higher inter-ensemble FRET in the latter, which is unchanged with time.

IV. CONCLUSIONS

Our results demonstrate that a specific combination of intra- and inter-ensemble ET between the QDs in the layers can greatly enhance the photo-stability of both sets of QDs. Low intra-ensemble FRET slows donor quench rate, which in turn allows the active donors to sustain moderate inter-ensemble FRET which keeps feeding carriers to the

acceptors, making them appear bright and stable. The segregated layered structure is of technical importance since such architecture is central to many QD-based applications, particularly for energy harvesting devices where directional energy transfer is vital. Understanding and characterizing the performance and stability metrics of these structures are therefore of considerable interest, and the results presented here suggest the layer geometry may be able to overcome some of the photo-induced issues typically observed in QD films, making this an optimal design for QD based devices.

ACKNOWLEDGMENTS

This research was partially supported by NSF CAREER DMR-1054161 and CAREER DMR-1056860. Portions of this work were performed at the Vanderbilt Institute of Nanoscale Science and Engineering, using facilities renovated under NSF ARI-R2 DMR-0963361.

[1]A. I. Ekimov and A. A. Onushchenko, JETP Lett. **34**, 0612 (1981). Available at http://www.jetpletters.ac.ru/ps/1517/article_23187.shtml
[2]R. Rossetti, J. L. Ellison, J. M. Gibson, and L. E. Brus, J. Chem. Phys. **80**, 4464 (1984).
[3]B. O. Dabbousi, J. Rodriguez-Viejo, F. V. Mikulec, J. R. Heine, H. Mattoussi, R. Ober, K. F. Jensen, and M. G. Bawendi, J. Phys. Chem. B **101**, 9463 (1997).
[4]N.-M. Park, T.-S. Kim, and J. Park, Appl. Phys. Lett. **78**, 2575 (2001).
[5]J. K. Jaiswal, H. Mattoussi, J. M. Mauro, and S. M. Simon, Nat. Biotechnol. **21**, 47 (2002).
[6]A. J. Nozik, Physica E **14**(1–2), 115 (2002).
[7]G. V. Shcherbatyuk, R. H. Inman, C. Wang, R. Winston, and S. Ghosh, Appl. Phys. Lett. **96**, 191901 (2010).
[8]W. G. J. H. M. van Sark, P. L. T. M. Frederix, D. J. Van den Heuvel, and H. C. Gerritsen, J. Phys. Chem. B **105**, 8281 (2001).
[9]S. R. Cordero, P. J. Carson, R. A. Estabrook, G. F. Strouse, and S. K. Buratto, J. Phys. Chem. B **104**, 12137 (2000).
[10]J. Aldana, Y. A. Wang, and X. Peng, J. Am. Chem. Soc. **123**, 8844 (2001).
[11]B. Mahler, P. Spinicelli, S. Buil, X. Quelin, J.-P. Hermier, and B. Dubertret, Nature Mater. **7**, 659 (2008).
[12]X. Cao, C. M. Li, H. Bao, Q. Bao, and H. Dong, Chem. Mater. **19**, 3773 (2007).
[13]D. G. Kim, S. Okahara, M. Nakayama, and Y. G. Shim, Phys. Rev. B **78**, 153301 (2008).
[14]G. V. Shcherbatyuk, R. H. Inman, and S. Ghosh, J. Appl. Phys. **110**, 053518 (2011).
[15]G. V. Shcherbatyuk, P. Talbot, and S. Ghosh, Appl. Phys. Lett. **100**, 212114 (2012).
[16]S. A. Hasan, D. W. Kavich, S. V. Mahajan, and J. H. Dickerson, Thin Solid Films **517**, 2665 (2009).
[17]S. A. Hasan, D. W. Kavich, and J. H. Dickerson, Chem. Commun. **25**, 3723 (2009).
[18]S. V. Mahajan, J. Cho, M. S. P. Shaffer, A. R. Boccaccini, and J. H. Dickerson, J. Eur. Ceram. Soc. **30**, 1145 (2010).
[19]S. V. Mahajan, S. A. Hasan, J. Cho, M. S. P. Shaffer, A. R. Boccaccini, and J. H. Dickerson, Nanotechnology **19**, 195301 (2008).
[20]S. F. Lee and M. A. Osborne, ChemPhysChem **10**, 2174 (2009).
[21]S. Maenosono, Chem. Phys. Lett. **376**, 666 (2003).
[22]H. Asami, Y. Abe, T. Ohtsu, I. Kamiya, and M. Hara, J. Phys. Chem. B **107**, 12566 (2003).
[23]H. Bao, Y. Gong, Z. Li, and M. Gao, Chem. Mater. **16**, 3853 (2004).
[24]J. A. Kloepfer, S. E. Bradforth, and J. L. Nadeau, J. Phys. Chem. B **109**, 9996 (2005).
[25]A. J. Krejci, C. G. W. Thomas, and J. H. Dickerson, Phys. Rev. E **87**, 042307 (2013).
[26]D. He, N. N. Ekere, and L. Cai, Mater. Sci. Eng., A **298**, 209 (2001).
[27]R. A. Quinn, C. Cui, J. Goree, J. B. Pieper, H. Thomas, and G. E. Morfill, Phys. Rev. E **53**, R2049 (1996).
[28]P. J. Steinhardt, D. R. Nelson, and M. Ronchetti, Phys. Rev. B **28**, 784 (1983).
[29]F. H. Kaatz, A. Bultheel, and T. Egami, Naturwiss. **95**, 1033 (2008).
[30]C. D. F. Rogers, T. A. Dijkstra, and I. J. Smalley, Earth-Sci. Rev. **36**, 59 (1994).
[31]A. J. Krejci, C. G. W. Thomas, J. Mandal, I. Gonzalo-Juan, W. He, R. L. Stillwell, J.-H. Park, D. Prasai, V. Volkov, K. I. Bolotin, and J. H. Dickerson, J. Phys. Chem. B **117**, 1664 (2013).
[32]S. K. Goswami, T. S. Kim, E. Oh, K. K. Challa, and E.-T. Kim, AIP Adv. **2**, 032132 (2012).
[33]M. Lunz, A. Louise Bradley, V. A. Gerard, S. J. Byrne, Y. K. Gun'ko, V. Lesnyak, and N. Gaponik, Phys. Rev. B **83**, 115423 (2011).